electronics

MDPI

Article

A Data-Driven Motor Optimization Method Based on Support Vector Regression—Multi-Objective, Multivariate, and with a Limited Sample Size

Guanghao Li, Ruicheng Li, Haobo Hou, Guoyi Zhang and Zhiyong Li *

School of Automation, Central South University, Changsha 410083, China; 8207210205@csu.edu.cn (G.L.); 8207210202@csu.edu.cn (R.L.); 8207211930@csu.edu.cn (H.H.); 8207211731@csu.edu.cn (G.Z.)
* Correspondence: lizy@csu.edu.cn

Abstract: The increasing demand for sustainable development and energy efficiency underscores the importance of optimizing motors in driving the upgrade of energy structures. This paper studies a data-driven approach for the multi-objective optimization of motors designed for scenarios involving multiple variables, objectives, and limited sample sizes and validates its efficacy. Initially, sensitivity analysis is employed to identify potentially influential variables, thus selecting key design parameters. Subsequently, Latin hypercube sampling (LHS) is utilized to select experimental points, ensuring the coverage of the modeled test points across the experimental space to enhance fitting accuracy. Finally, the support vector regression (SVR) algorithm is employed to fit the objective function, in conjunction with multi-objective particle swarm optimization (MOPSO) for solution derivation. The presented method is used to optimize the efficiency, average output torque, and induced electromotive force harmonic distortion rate of a permanent magnet synchronous motor (PMSM). The results show an improvement of approximately 6.80% in average output torque and a significant decrease of about 59.5% in the induced electromotive force harmonic distortion rate, with minimal impact on efficiency. This study offers a pathway for enhancing motor performance, holding practical significance.

Keywords: multi-objective optimization of motors; data drive; support vector regression (SVR); Latin hypercube sampling (LHS)

check for updates

Citation: Li, G.; Li, R.; Hou, H.; Zhang, G.; Li, Z. A Data-Driven Motor Optimization Method Based on Support Vector Regression—Multi-Objective, Multivariate, and with a Limited Sample Size. *Electronics* **2024**, *13*, 2231. https://doi.org/10.3390/electronics13122231

Academic Editor: Jianguo Zhu

Received: 4 April 2024
Revised: 24 May 2024
Accepted: 4 June 2024
Published: 7 June 2024

Copyright: © 2024 by the authors. Licensee MDPI, Basel, Switzerland. This article is an open access article distributed under the terms and conditions of the Creative Commons Attribution (CC BY) license (https://creativecommons.org/licenses/by/4.0/).

1. Introduction

Given its central role in energy systems, the optimization of motor performance emerges as paramount, influencing the efficacy of the entire energy system [1,2].

Currently, prevalent modeling approaches for motor optimization encompass both model-driven and data-driven methodologies. Model-driven modeling relies on fundamental electromagnetic principles to construct motor models [3–6], while data-driven methods leverage observed motor performance data and employ statistical and machine learning techniques to unveil system patterns and relationships [7–9]. Employing data-driven methodologies to establish mathematical models for motors offers advantages such as reduced computational complexity and robust generalization capabilities [5,10,11]. Moreover, data-driven techniques harness machine learning methodologies to better capture the intricacies of complex systems [12].

Data-driven approaches have yielded significant advancements in the realm of motor optimization. A multi-tiered optimization strategy, integrating fuzzy reasoning with sequential Taguchi methodology, has demonstrated enhanced optimization precision for IPMSMs [13]. A fuzzy sequential Taguchi method is utilized to achieve efficient and robust design optimization of fault tolerance for five-phase in-wheel motors of electric vehicles [14]. Employing a combination of particle swarm optimization with a response surface method has proven effective in optimizing output torque and cogging torque of transverse flux permanent magnet motors [15]. Online data-driven methodologies leveraging dual-loop

optimization have streamlined the optimization process for permanent magnet linear synchronous motors [16]. Optimization efforts for interior permanent magnet synchronous motors within hub motors, utilizing a Kriging model based on Latin hypercube sampling, have achieved a broader speed range and reduced cogging torque [17]. The optimization of average thrust and thrust ripple for double-layered flux-switching permanent magnet motors was successfully realized through a hybrid approach, integrating random forest optimization of hyperparameters with non-dominated sorting genetic algorithm-II (NSGA-II) [18]. The utilization of a proxy model based on DNN has facilitated the optimization of rotor torque and mechanical stress for motors [19].

Data-driven motor modeling also presents some noteworthy issues. Reference [20] highlights that the complexity of the motor optimization process increases with multidimensional design variables, thus necessitating a reduction in design space. Reference [21] points out the curse of dimensionality in data-driven modeling with high-dimensional data, manifested in sparse data distributions and the trend toward the edges of the space. To ensure the accuracy of regression models, reference [22] achieves effective sparsity structures by developing a G-group-level parameter inference GRIP test through assumed formulations.

The experimental cost of obtaining samples for data-driven motor optimization is relatively high, often resulting in limited data scale [23]. Reference [24] indicates that when modeling with small sample sizes and high-dimensional data, estimates of model parameters may be biased, leading to reduced prediction accuracy. Reference [25] discusses the influence of data dimensionality and sample size on the performance of machine learning models. Reference [26] suggests that machine learning methods are an effective means of addressing challenges in modeling with small data samples.

In engineering practice, the selection of suitable Pareto frontier optimal solutions requires consideration of multiple factors, including technical feasibility and cost-effectiveness. It entails not only guidance from scientific theories but also practical experience and skills [27]. Reference [28] emphasizes the potentially vast size of the Pareto solution set, underscoring the critical importance of judiciously selecting Pareto solutions for the quality and practicality of optimization outcomes. Reference [29] introduces a quantitative approach to evaluating Pareto solutions by establishing the average variability of objective function values associated with adjacent Pareto solutions. Additionally, reference [30] employs the R-method to rank Pareto optimal solutions.

Given the complexity of electric motors as intricate systems and the constraints posed by experimental costs, optimizing electric motors using data-driven approaches presents the characteristics as multivariate, multi-objectivity, and small dataset size. Prior research underscores the importance of conducting sensitivity analyses on motor design variables to mitigate the curse of dimensionality during modeling processes. In practical terms, owing to limited dataset sizes and high experimental costs, ensuring that the experimental points adequately cover the design space under constrained scales is imperative to ensure modeling accuracy. Additionally, attention must be paid to selecting Pareto-optimal solutions, as this impacts the quality and practicality of optimization outcomes. When addressing electric motor optimization problems, a comprehensive consideration of multiple factors is essential to derive reliable and practical optimization solutions.

Within this study, we aim to explore a data-driven approach for optimizing motor design, capitalizing on the inherent advantages of data-driven methodologies to enhance various facets of motor performance, including efficiency, output torque, and induced electromotive force. To elucidate and substantiate our proposed methodology, we initially focus on a permanent magnet synchronous motor as our optimization target, with efficiency, average torque, and harmonic distortion of induced electromotive force serving as our optimization objectives. Leveraging pre-existing knowledge, we conduct sensitivity analyses on key motor parameters, retaining sensitive variables as design parameters to effectively streamline the design space. Subsequently, we employ Latin hypercube sampling based on the Morris–Mitchell criterion to design the experimental space, ensuring comprehensive spatial coverage of the dataset. Following this, we utilize support vector regression (SVR)

to construct the motor model based on a relatively modest dataset. Lastly, we integrate a multi-objective particle swarm optimization algorithm to yield non-dominated solutions. Given the complexities and constraints inherent in engineering implementations, we adopt the principle of proximity to select Pareto-optimal solutions and compare performance metrics both pre- and post-optimization. The flowchart of this study is delineated in Figure 1.

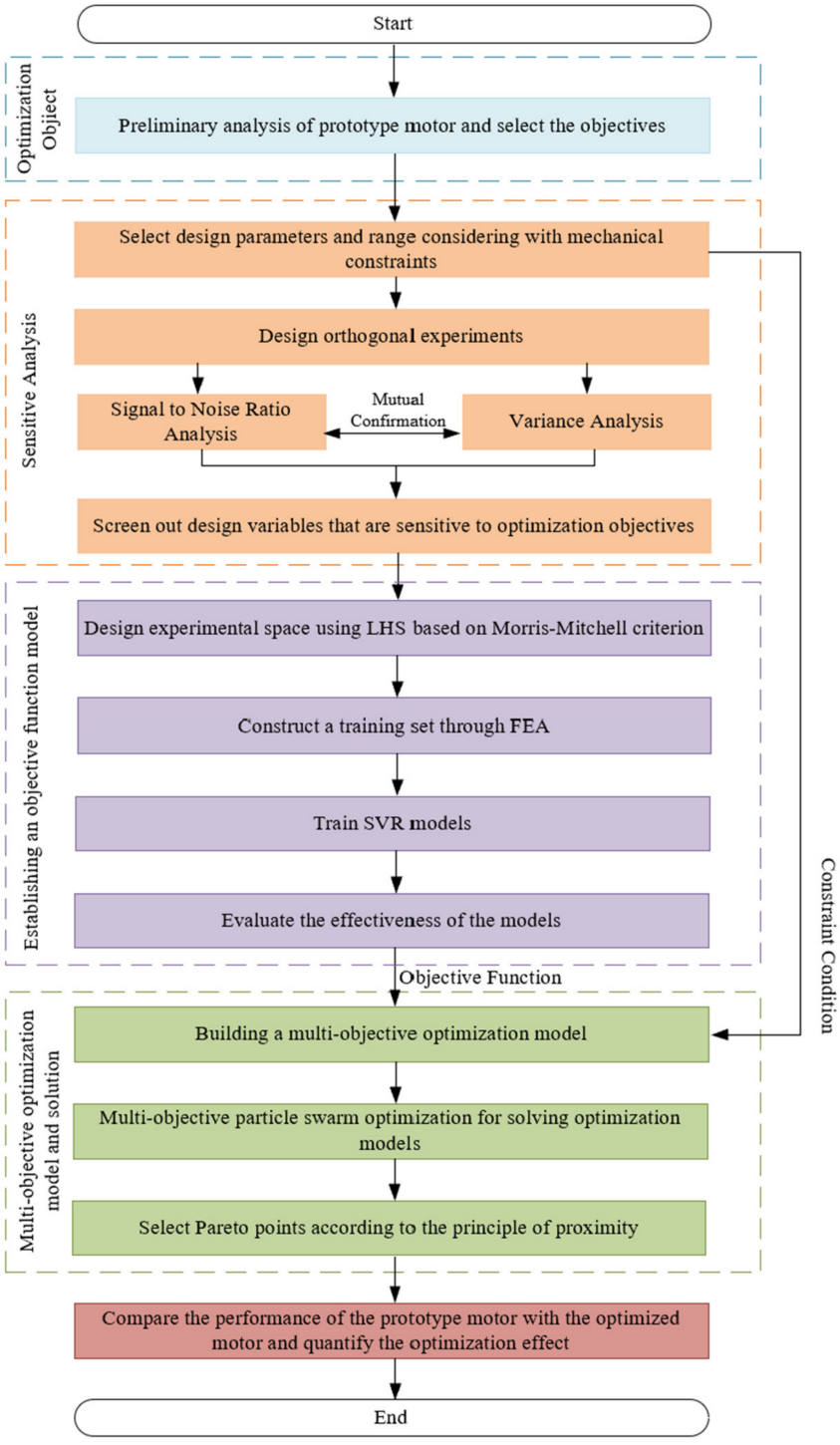


Figure 1. The flowchart of this study.

2. Prototype Model

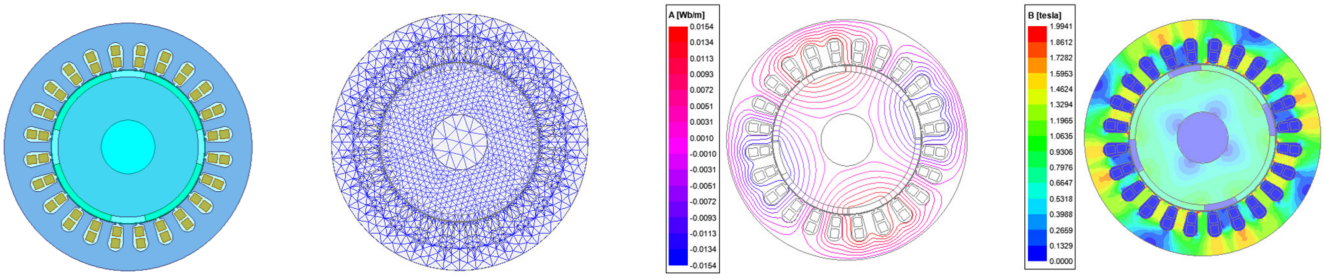
This paper focuses on optimizing a surface-mounted PMSM, targeting efficiency, average torque, and harmonic distortion of the electromotive force as optimization objectives. The motor parameters are outlined in Table 1.

Table 1. Parameters of PMSM.

Parameter Value	Value
Material of stator core	Silicon steel sheet
Material of rotor core	Silicon steel sheet
Material of stator conductor	Copper
Inner diameter of rotor	74 mm
Outer diameter of stator	120 mm
Effective length of motor	65 mm
Air gap length	0.5 mm
PM thickness	3 mm
Pole arc coefficient of PM	0.7
Width of stator slot	2.5 mm
Height of stator slot	0.5 mm

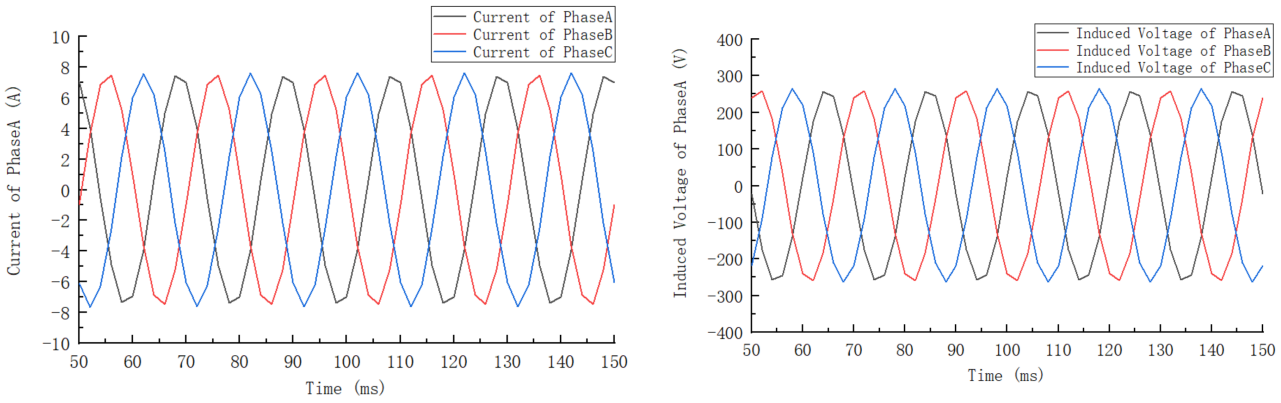
Finite element analysis was conducted using ANSYS Maxwell 2020R1 software. Motor parameters were inputted to construct the computer model. The motor operates at a synchronous speed of 1500 rpm with a power angle of 8.7°. It has a rated phase voltage of 220 V, winding resistance of 10 Ω, and winding self-inductance of 5.13 mH. Simulation time spans 200 ms, with a 2 ms time step.

Figure 2a illustrates the motor model within ANSYS Maxwell, while Figure 2b displays the mesh partition, indicating reasonable division. Figure 2c exhibits magnetic flux lines, showcasing satisfactory closure and symmetry with minimal leakage flux. Figure 2d demonstrates magnetic flux density contours, with peak density near the air gap reaching approximately 2 T. Figure 3a portrays phase current waveforms, reflecting good symmetry and stable amplitude across the three phases. Lastly, Figure 3b depicts phase voltage waveforms of induced electromotive force, also demonstrating favorable symmetry and stable amplitude across phases.



(**a**) (**b**) (**c**) (**d**)

Figure 2. The FEA model of the prototype motor: (**a**) model in ANSYS Maxwell; (**b**) grid division diagram; (**c**) magnetic field line; and (**d**) magnetic flux density cloud map.



(**a**) (**b**)

Figure 3. Preliminary analysis of the prototype motor: (**a**) phase current waveform; (**b**) induced electromotive force phase voltage waveform.

3. Variable Sensitivity Analysis

The objective of variable sensitivity analysis is to evaluate the impact of variables on model outputs, assisting in the identification of the most influential variables and those that can be omitted, thereby reducing the dimensionality of input variables in modeling with minimizing any potential reduction in model accuracy.

3.1. Common Design Variables and Optimization Objectives

Drawing upon prior knowledge in motor engineering, it is recognized that the air gap length, permanent magnet thickness, permanent magnet pole arc coefficient, and stator slot dimensions, especially the slot width and height, exert influence on the efficiency, output torque, and induced electromotive force of the motor [31–36].

Selected design variables for the motor include air gap length, permanent magnet thickness, permanent magnet pole arc coefficient, stator slot width, and stator slot height. Optimization objectives encompass motor efficiency, average torque, and harmonic distortion of the induced electromotive force. The symbols representing design variables and optimization objectives are outlined in Table 2.

Table 2. Symbols for design variables and optimization objectives.

	Factor	Symbol	Unit
Design Variables	Air gap length	δ	mm
	PM thickness	d_m	mm
	Pole arc coefficient of PM	a_m	/
	Width of stator slot	b_{s0}	mm
	Height of stator slot	h_{s0}	mm
Optimization Objectives	Motor efficiency	η	/
	Average output torque	T_{av}	N·m
	Induced electromotive force harmonic distortion rate	THD_u	/

3.2. Sensitivity Analysis Experiment

The sensitivity analysis test utilizes the orthogonal test method, which is an experimental design approach that examines various factors and levels [11,37]. Signal-to-noise ratio analysis and variance analysis are conducted without the need to cover the entire test space. By using orthogonal tables to organize test plans and analyze results, orthogonal experiments can create efficient and representative test plans with minimal tests. Through the data obtained from these tests, the sensitivity of each factor is analyzed [38].

Table 3 presents the initial values of each design variable, which are the values of the design variables in the unoptimized prototype. In this study, although we are optimizing only five variables, it is essential to consider other aspects of motor performance and the rationality of various electromagnetic structural parameters. We defined a relatively reasonable range based on the initial levels of these five main electromagnetic structures, where the design variables should encompass their initial values. Then, we evenly sampled five points within these ranges as the five levels of each design variable. Based on these levels, we constructed an $L_{25}(5^5)$ orthogonal table. The five factors and their corresponding levels are outlined in Table 4.

Table 3. Benchmark level for optimizing variables.

Factor	Unit	Benchmark Level
δ	mm	0.50
d_m	mm	3.00
a_m	/	0.70
b_{s0}	mm	1.50
h_{s0}	mm	0.50

Table 4. Five experimental factors and their levels.

Factor	Unit	Level 1	Level 2	Level 3	Level 4	Level 5
δ	mm	0.40	0.45	0.50	0.55	0.60
d_m	mm	2.00	2.50	3.00	3.50	4.00
a_m	/	0.60	0.65	0.70	0.75	0.80
b_{s0}	mm	1.00	1.25	1.50	1.75	2.00
h_{s0}	mm	0.40	0.45	0.50	0.55	0.60

3.3. Signal to Noise Ratio Analysis and Variance Analysis

A table with 25 groups of test data was created, with five electromagnetic structure parameters input into ANSYS Maxwell for parametric simulation. This allowed for the calculation of motor efficiency, average torque, and electromotive force harmonics for each group. Subsequently, signal-to-noise ratio analysis and variance analysis on the motor efficiency, average torque, and electromotive force harmonic distortion rate based on the five electromagnetic structure parameters were conducted. Sensitivity curves were then plotted. The signal-to-noise ratio was first analyzed for each level of every factor using the calculation formula provided.

$$t = \frac{\overline{X}_i - \overline{X}}{\sqrt{\frac{s_i^2}{n_i} + \frac{s^2}{n}}} \tag{1}$$

where t denotes the signal-to-noise ratio for the factor at the ith level; $\overline{X_i}$ represents the mean of the dependent variable at the i-th level of the factor; $\overline{X}$ signifies the mean of the dependent variable across all levels of the factor; s_i indicates the variance of the dependent variable at the i-th level of the factor; s reflects the variance of the dependent variable across all levels of the factor; n_i stands for the degrees of freedom for the factor at the i-th level; and n represents the degrees of freedom for the factor across all levels.

Figure 4 illustrates the signal-to-noise ratio curves of motor efficiency, average torque, and harmonic distortion of induced electromotive force at various levels of each factor.

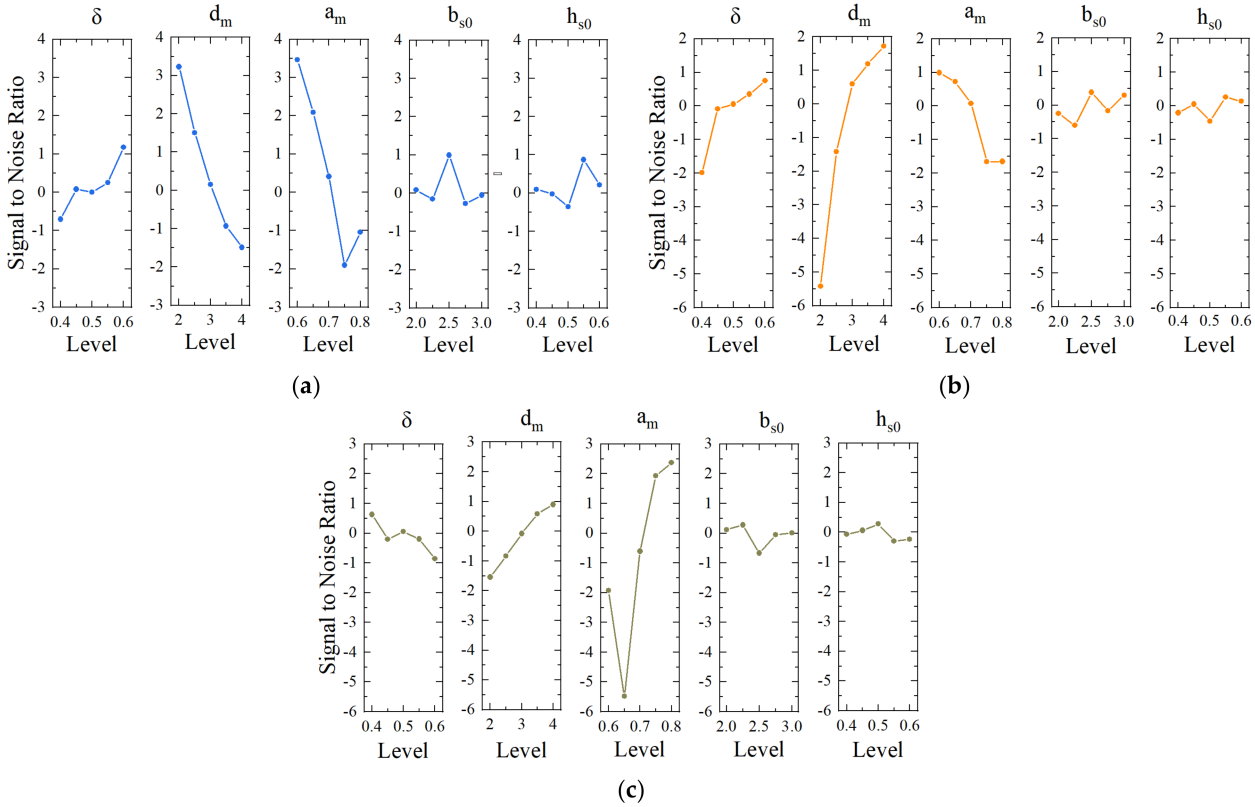


Figure 4. Signal-to-noise ratio curve: (**a**) signal-to-noise ratio analysis of motor efficiency; (**b**) signal-to-noise ratio analysis of average torque; and (**c**) signal-to-noise ratio analysis of electromotive force harmonic distortion rate.

To quantitatively analyze the respective impact of each factor on motor efficiency, average torque, and harmonic distortion of induced electromotive force of the PMSM, a variance analysis was conducted on the five factors (Table 5). This involved calculating the variance value for each factor. The formula for variance calculation is as follows:

$$\begin{cases} SSX = \sum_{i=1}^{n} [m_{X_i}(Y) - m(Y)]^2 \\ m_{X_i}(Y) = \frac{m}{n} \sum_{k=1}^{n} Y_k \\ m(Y) = \frac{1}{n} \sum_{j=1}^{n} Y_j \end{cases} \quad (2)$$

where n represents the number of tests; m represents the number of factor levels; X irepresents the experimental factor; Y represents the average value; $m_{X_i}(Y)$ represents the average value of Y at the i-th level of the X factor; and $m(Y)$ represents the average value of Y for all levels of all factors.

Table 5. Table of variance analysis.

Factor	η		T_{av}		THD_u	
	SSX	**Proportion**	**SSX**	**Proportion**	**SSX**	**Proportion**
δ	0.0008	0.0878	0.0642	0.1265	0.0039	0.0633
d_m	0.0037	0.4093	0.2927	0.5769	0.0111	0.1776
a_m	0.0042	0.4544	0.1267	0.2496	0.0457	0.7318
b_{s0}	0.0002	0.0221	0.0163	0.0320	0.0009	0.0140
h_{s0}	0.0002	0.0264	0.0076	0.0150	0.0008	0.0133

The results of signal-to-noise ratio analysis and variance analysis indicate that the stator slot width and slot height are not highly sensitive to the three optimization goals. The air gap length shows similar sensitivity to the three optimization goals, while the thickness of the permanent magnet significantly impacts motor efficiency and the average output torque with high sensitivity. Additionally, the polar arc coefficient of the permanent magnet has a notable effect on the harmonic distortion rate of the induced electromotive force. It is evident that different performance indicators of motors have varying high-sensitivity factors, necessitating careful consideration. In this study, the air gap length, permanent magnet thickness, and permanent magnet polar arc coefficient are chosen as optimization variables for further analysis to determine the best combination through an optimization algorithm.

4. Model Establishment

In data-driven motor optimization design, data processing determines the accuracy of the model and the effectiveness of the optimization. Through the improved Latin hypercube sampling method, a test space uniformly distributed in three-dimensional space was obtained. The data were input into ANSYS Maxwell. and a series of corresponding values of δ, d_m, a_m and η, T_{av}, $THDu$ were obtained. These data are used as training sets, and the support vector regression algorithm is used to construct the functional relationships between δ, d_m, a_m and η, T_{av}, $THDu$, respectively.

4.1. Design of Experimental Space for Modeling

The objective of experimental space design is to adequately capture the features of the system model using a limited number of sample data. This includes understanding the coupling relationship between variables and the mapping between design variables and target variables. Therefore, it is imperative that the experimental points effectively cover the experimental space to ensure the precision of fitting the objective function by the machine learning model.

Latin hypercube sampling (LHS) is a stratified sampling method that efficiently distributes samples throughout the experimental space, requiring fewer samples than traditional random sampling methods [39]. However, in ordinary Latin hypercube sampling, random arrangement of sample points may lead to suboptimal spatial coverage. To address this, the maximum–minimum distance criterion was introduced to enhance the spatial coverage of sampling points [40].

Morris and Mitchell extended the maximum–minimum distance criterion and proposed the ϕ_p criterion, also known as the Morris–Mitchell criterion [41]. An experimental design is called ϕ_p. An optimal design should satisfy the following conditions:

$$\min\{\phi_p\} = \min\left\{\left(\sum_{i=1}^{s} J_i d_i^{-p}\right)^{\frac{1}{p}}\right\}. \tag{3}$$

A smaller value of ϕ_p indicates better test sample space filling performance. In a specific test plan, the distance d_{ij} between any two sample points is sorted to create a list $(d_1, d_2, \ldots, d_s)$ along with the corresponding index list $(J_1, J_2, \ldots, J_s)$. Here, d_i represents different distance values, J_i represents the number of point pairs with distance d_i, s is the total number of different distance values, and p is a positive integer setting as 50.

The training set size required for this study is 200. Utilizing the Latin hypercube sampling method based on the Morris–Mitchell criterion, we acquired a set of 200 sampling points with good coverage in the three-dimensional space. By inputting the data from these sampling points into ANSYS Maxwell for analysis, we can derive both the training and testing sets for the model. The spatial distribution of the sampling points is depicted in Figure 5.

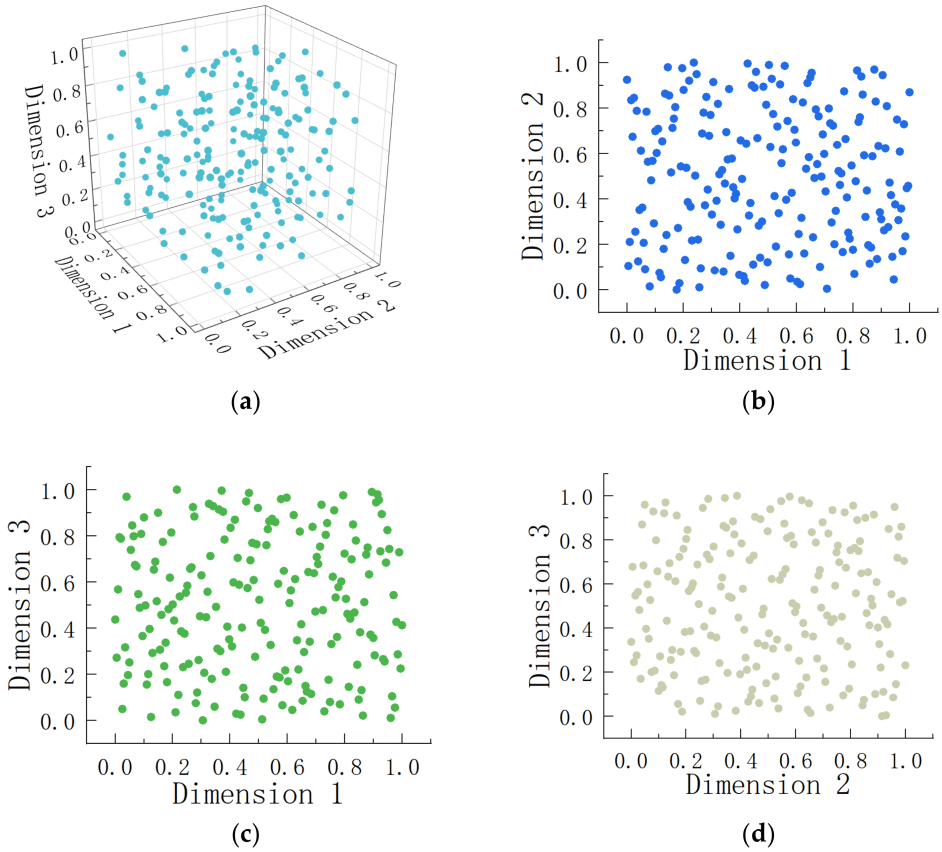


Figure 5. The sampling results of improving Latin hypercube: (**a**) 3D images of the experimental space; (**b**) projection of experimental points on Dimension 1 and Dimension 2; (**c**) projection of experimental points on Dimension 1 and Dimension 3; (**d**) projection of experimental points on Dimension 2 and Dimension 3.

4.2. Modeling Based on Support Vector Regression

Selecting support vector regression (SVR) to model the objective function of the motor is recommended. Support vector machines typically outperform other models in small sample datasets [42,43], efficiently handle data in high-dimensional space, and address linearly inseparable situations through kernel functions, showcasing strong generalization capabilities. The fundamental concept of SVR is to identify a hyperplane that minimizes the distance between sample points and the hyperplane within a specified tolerance.

For a given training dataset $\{(x_1, y_1), (x_2, y_2), \ldots, (x_n, y_n)\}$, where x_1 represents the input feature and y_1 is the corresponding output, the objective of support vector regression (SVR) is to determine a function $f(x)$ that can predict the output y for a new input x. The model expression for SVR is as follows:

$$f(x) = \langle w, x \rangle + b. \tag{4}$$

Here, w is the weight vector, b is the bias (intercept), and $\langle \cdot, \cdot \rangle$ represents the inner product. SVR utilizes a loss function to quantify the prediction error. In SVR, the loss function typically includes an error term along with a penalty term:

$$L(y, f(x)) = \max(0, |f(x) - y| - \xi). \tag{5}$$

The tolerance (ξ) in support vector regression (SVR) refers to the acceptable range of data points that can be considered as support vectors. It is a crucial parameter used to determine the level of deviation allowed for data points to be classified as support vectors.

The mathematical expression for SVR incorporates this tolerance to identify the support vectors within the specified range.

$$\begin{aligned} \text{min.} \quad & \tfrac{1}{2}\|w\|^2 + C\sum_{i=1}^{N}\xi_i \\ st. \quad & y_i(w \cdot x_i + b) \geq 1 - \xi_i, i = 1, 2, \cdots, N \\ & \xi_i \geq 0, i = 1, 2, \cdots, N \end{aligned} \tag{6}$$

where C is the regularization coefficient and N is the number of samples. The goal of this optimization problem is to find a maximum margin hyperplane while ensuring that all sample points satisfy the constrain.

At the same time, in order to achieve nonlinear fitting, kernel skill needs to be used. The SVR algorithm in this article uses a Gaussian kernel (RBF kernel). The expression of Gaussian kernel is as follows:

$$K(x_i, x_j) = e^{-\gamma\|x_i - x_j\|^2} \tag{7}$$

where γ defines the range of influence of a single sample, with smaller values indicating a smaller impact and larger values indicating a broader influence range. The parameter settings for the SVR algorithm in this study are presented in Table 6.

Table 6. Parameter settings for SVR algorithm.

Parameter	Value
Kernal Function Type	RBF
N	200
C	1
γ	0.5

4.3. Analysis of the Effect of Models Fitting

Utilizing support vector regression (SVR), the functions for δ, d_{mag}, a, η, T_{av}, and $THDu$ were fitted. The fitting performance is visually demonstrated in Figure 6. The test set data shows that all three functions effectively capture the patterns. Analysis from Table 7 reveals that the root mean square error (RMSE) for all three functions is minimal, while the R^2 Score is high, indicating a strong fitting performance.

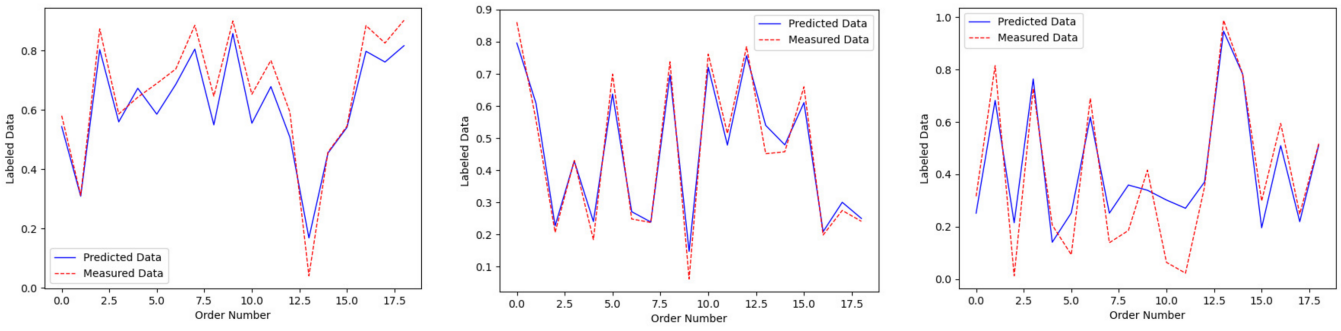


Figure 6. The effect of models fitting: (**a**) the performance of the model about η on the test set; (**b**) the performance of the model about T_{av} on the test set; (**c**) the performance of the model about $THDu$ on the test set.

Table 7. Score of models.

Factor	RMSE [1]	R^2 Score
η	0.0722	0.89
T_{av}	0.0454	0.96
THD_u	0.1028	0.84

[1] Root mean square error.

5. Multi-Objective Optimization Problems and Solutions

5.1. Multi-Objective Optimization Model

The independent variable column vector $x = [\delta, d_m, a_m]^T$ consists of the air gap length δ, permanent magnet thickness d_m, and permanent magnet polar arc coefficient a_m. The functions relating x to η, T_{av}, and $THDu$, obtained through SVR fitting, are $\eta = f_1(x)$, $T_{av} = f_2(x)$, and $THDu = f_3(x)$, respectively. Therefore, the multi-objective optimization model can be expressed as a relationship between x and these performance metrics.

$$\begin{aligned} \text{min.} \quad & -f_1(x) \\ & -f_2(x) \\ & f_3(x) \\ st. \quad & 0.4 \le \delta \le 0.6 \\ & 2 \le d_m \le 4 \\ & 0.6 \le a_m \le 0.8 \end{aligned} \tag{8}$$

5.2. Model Solutions

The optimization model is solved using a multi-objective particle swarm optimization algorithm. Multi-objective particle swarm optimization (MOPSO) is a meta-heuristic optimization algorithm utilized for solving multi-objective optimization problems. The fundamental concept involves treating each solution as a particle and simulating particle behavior within the population to systematically explore the solution space and identify the Pareto front, which represents the optimal solutions [44]. The parameter settings of the particle swarm optimization algorithm used in this study are shown in Table 8.

Table 8. Parameter settings for MOPSO algorithm.

Parameter	Value
Number of iterations terminated	100
Particle swarm size	100
Non-dominated solution scale	100
Particle size	3
Particle velocity	−0.2~0.2
Number of grids divided	2500

The multi-objective optimization model described can be effectively addressed with the multi-objective particle swarm algorithm. The Pareto solutions are presented in Table 9, and the fitness Pareto frontier image is depicted in Figure 7.

Table 9. Pareto solution set.

η	T_{av}	THD_u
0.4235	0.6400	2.703
0.5114	0.6534	3.222
0.5362	0.6006	3.715
...	...	...

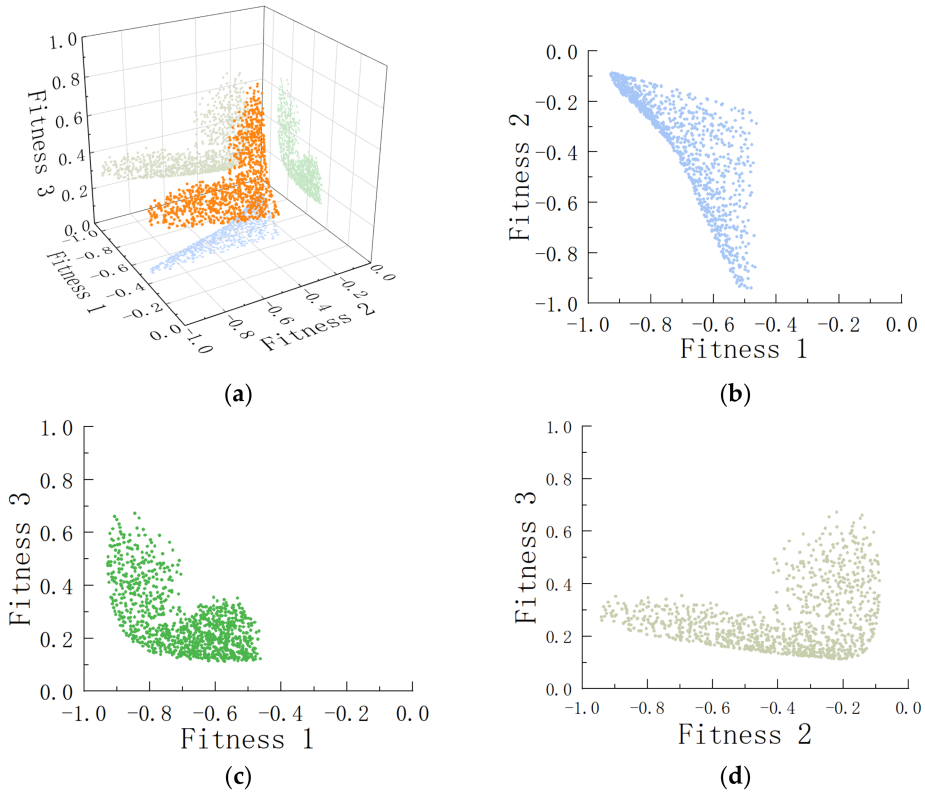


Figure 7. Pareto frontier images: (**a**) Pareto frontier 3D images; (**b**) projection of Pareto frontier on Fitness 1 and Fitness 2; (**c**) projection of Pareto frontier on Fitness 1 and Fitness 3; (**d**) projection of Pareto frontier on Fitness 2 and Fitness 3.

In the figure, Fitness 1 represents the fitness value for δ, Fitness 2 represents the fitness value for d_m, and Fitness 3 represents the fitness value for a_m. The Pareto relationship between motor efficiency and average output torque shows an approximate linear relationship with a negative correlation. Similarly, the Pareto relationship between efficiency and the harmonic distortion rate of induced electromotive force exhibits a hyperbolic relationship with a negative correlation. The average output torque and induced electromotive force display a Pareto relationship with harmonic distortion rates, presenting a transcendental function relationship.

The selection of Pareto-optimal solutions requires consideration of both scientific validity and engineering practicality [27]. When choosing Pareto-optimal solutions, it is crucial to ensure their scientific validity, meaning they are derived through reliable methods and techniques. In engineering practice, selecting Pareto-optimal solutions close to the prototype offers advantages. This is because solutions close to the prototype suggest that the manufacturing challenges are similar to those of the prototype, thereby reducing uncertainty and risk during the actual production process. Furthermore, solutions close to the prototype typically do not necessitate additional productive research and development or adjustments, resulting in time and cost savings. Utilizing the proximity principle, a Pareto solution near the parameter structure before optimization was selected: $\delta = 0.5114$, $d_m = 3.222$, $a_m = 0.6534$. The improvement of motor performance before and after optimization was then compared (Table 10).

Table 10. Comparison of motor performance before and after optimization.

	η	T_{av}	THD_u
Before optimization	0.9564	3.5080	0.1793
After optimization	0.9537	3.7465	0.0726

The optimization solutions resulted in an approximately 6.80% increase in the average output torque of the motor. This improvement can be attributed to a reduction in the air gap of the motor, leading to decreased reluctance and increased magnetic density, ultimately boosting the output torque. Additionally, the harmonic distortion rate of the induced electromotive force decreased by around 59.5%. This reduction was achieved by adjusting the thickness of the permanent magnet and the polar arc coefficient, resulting in a magnetic field closer to a sine wave and reducing harmonic components. However, there was a slight decrease of about 0.282% in motor efficiency, primarily due to the decrease in the polar arc coefficient of the permanent magnet, leading to a decrease in the winding magnetic flux. Overall, with allowable errors, it can be considered that the efficiency of the motor has hardly decreased, while the improvement in average output torque and harmonic distortion rate indicates that the motor performance has been enhanced. It can be concluded that this optimization method has effectively enhanced the motor's performance.

6. Conclusions

Through this study, we have explored a data-driven approach to motor optimization, aiming to tackle the challenges posed by multiple objectives, variables, and small sample sizes. Our objective is to achieve more accurate data-driven modeling and optimize motor performance effectively.

Our methodology involves a targeted selection of key parameters through sensitivity analysis, leading to a reduction in the dimensionality of the design variable space. This step enhances optimization efficiency and accuracy. Additionally, we employ Latin hypercube sampling based on the Morris–Mitchell criterion to systematically design experimental spaces for establishing optimization models. Leveraging support vector regression, we develop a more precise surrogate model of the motor based on a small sample size. Finally, considering the practical difficulties and constraints of engineering implementation, we adopt a nearest-neighbor approach to select a set of Pareto front optimal solutions.

Utilizing the approach detailed in this study, we targeted a permanent magnet synchronous motor for optimization, focusing on efficiency, average output torque, and harmonic distortion of the induced electromotive force. Through our optimization methodology, we achieved a notable 6.80% increase in average output torque and successfully reduced the harmonic distortion of the induced electromotive force by 59.5% while maintaining near-constant motor efficiency.

In conclusion, this study presents a method and technology for motor optimization design, offering robust support for enhancing motor performance and achieving more efficient energy utilization.

Author Contributions: Conceptualization, G.L. and Z.L.; methodology, G.L. and R.L.; software, G.L. and G.Z.; validation, G.L. and R.L.; formal analysis, H.H.; investigation, H.H. and G.L.; resources, Z.L.; data curation, G.L.; writing—original draft preparation, G.L.; writing—review and editing, Z.L.; visualization, R.L. and G.L.; supervision, Z.L.; project administration, G.L. All authors have read and agreed to the published version of the manuscript.

Funding: This research received no external funding.

Data Availability Statement: Data are contained within the article.

Conflicts of Interest: The authors declare no conflicts of interest.

References

1. Bazmi, A.A.; Zahedi, G. Sustainable Energy Systems: Role of Optimization Modeling Techniques in Power Generation and Supply—A Review. *Renew. Sustain. Energy Rev.* **2011**, *15*, 3480–3500. [CrossRef]
2. Zhu, X.; Fan, D.; Xiang, Z.; Quan, L.; Hua, W.; Cheng, M. Systematic Multi-Level Optimization Design and Dynamic Control of Less-Rare-Earth Hybrid Permanent Magnet Motor for All-Climatic Electric Vehicles. *Appl. Energy* **2019**, *253*, 113549. [CrossRef]
3. Lu, C.; Yang, Z.; Sun, X.; Ding, Q. Design and Multi-Objective Optimization of a Composite Cage Rotor Bearingless Induction Motor. *Electronics* **2023**, *12*, 775. [CrossRef]

4. Yu, S.; Zhou, Y.; Wang, Y.; Zhang, J.; Dong, Q.; Tian, J.; Chen, J.; Leng, F. Optimization Study of Cooling Channel for the Oil Cooling Air Gap Armature in a High-Temperature Superconducting Motor. *Electronics* **2024**, *13*, 97. [CrossRef]
5. Li, M.; Chen, Z.; Mu, H.; Lun, S. Synergistic Optimization Design Method to Improve the Overload Capacity and Efficiency of Canned Permanent Magnet Synchronous Motor for Vacuum Pump. *Electronics* **2023**, *12*, 4631. [CrossRef]
6. Mei, J.; Zuo, Y.; Lee, C.H.T.; Kirtley, J.L. Modeling and Optimizing Method for Axial Flux Induction Motor of Electric Vehicles. *IEEE Trans. Veh. Technol.* **2020**, *69*, 12822–12831. [CrossRef]
7. Cen, J.; Yang, Z.; Liu, X.; Xiong, J.; Chen, H. A Review of Data-Driven Machinery Fault Diagnosis Using Machine Learning Algorithms. *J. Vib. Eng. Technol.* **2022**, *10*, 2481–2507. [CrossRef]
8. Gou, B.; Xu, Y.; Xia, Y.; Wilson, G.; Liu, S. An Intelligent Time-Adaptive Data-Driven Method for Sensor Fault Diagnosis in Induction Motor Drive System. *IEEE Trans. Ind. Electron.* **2019**, *66*, 9817–9827. [CrossRef]
9. Alsina, E.F.; Chica, M.; Trawiński, K.; Regattieri, A. On the Use of Machine Learning Methods to Predict Component Reliability from Data-Driven Industrial Case Studies. *Int. J. Adv. Manuf. Technol.* **2018**, *94*, 2419–2433. [CrossRef]
10. Li, G.; Sun, H.; Hu, W.; Li, Y.; Bai, Y.; Guo, Y. Multi-Objective Optimization Design of the External Rotor Permanent Magnet-Assisted Synchronous Reluctance Motor Based on the Composite Algorithm. *Electronics* **2023**, *12*, 4004. [CrossRef]
11. Sun, H.; Li, Y.; Zhang, L.; Xue, Z.; Hu, W.; Li, G.; Guo, Y. Multi-Parameter Optimization of Stator Coreless Disc Motor Based on Orthogonal Response Surface Method. *Electronics* **2023**, *12*, 3020. [CrossRef]
12. Akbar, K.; Zou, Y.; Awais, Q.; Baig, M.J.A.; Jamil, M. A Machine Learning-Based Robust State of Health (SOH) Prediction Model for Electric Vehicle Batteries. *Electronics* **2022**, *11*, 1216. [CrossRef]
13. Sun, X.; Shi, Z.; Zhu, J. Multiobjective Design Optimization of an IPMSM for EVs Based on Fuzzy Method and Sequential Taguchi Method. *IEEE Trans. Ind. Electron.* **2021**, *68*, 10592–10600. [CrossRef]
14. Shi, Z.; Sun, X.; Cai, Y.; Yang, Z. Robust Design Optimization of a Five-Phase PM Hub Motor for Fault-Tolerant Operation Based on Taguchi Method. *IEEE Trans. Energy Convers.* **2020**, *35*, 2036–2044. [CrossRef]
15. Zhang, C.; Chen, Z.; Mei, Q.; Duan, J. Application of Particle Swarm Optimization Combined With Response Surface Methodology to Transverse Flux Permanent Magnet Motor Optimization. *IEEE Trans. Magn.* **2017**, *53*, 1–7. [CrossRef]
16. Liu, X.; Hu, C.; Li, X.; Gao, J.; Huang, S. An Online Data-Driven Multi-Objective Optimization of a Permanent Magnet Linear Synchronous Motor. *IEEE Trans. Magn.* **2021**, *57*, 1–4. [CrossRef]
17. Kim, J.B.; Hwang, K.Y.; Kwon, B.I. Optimization of Two-Phase In-Wheel IPMSM for Wide Speed Range by Using the Kriging Model Based on Latin Hypercube Sampling. *IEEE Trans. Magn.* **2011**, *47*, 1078–1081. [CrossRef]
18. Wen, C.; Zhao, Q.; Li, M.; Liu, J.; Li, M.; Zhao, X. Multi-Objective Optimization Based on Hyperparameter Random Forest Regression for Linear Motor Design. *Int. J. Mach. Learn. Cybern.* **2022**, *13*, 2929–2942. [CrossRef]
19. Barmada, S.; Tucci, M.; Sani, L.; Tozzo, C. Deep Neural Network-Based Electro-Mechanical Optimization of Electric Motors. *IEEE Trans. Magn.* **2023**, *59*, 1–4. [CrossRef]
20. Duan, Y.; Ionel, D.M. A Review of Recent Developments in Electrical Machine Design Optimization Methods With a Permanent-Magnet Synchronous Motor Benchmark Study. *IEEE Trans. Ind. Appl.* **2013**, *49*, 1268–1275. [CrossRef]
21. Jiang, X.; Kong, X.; Ge, Z. Augmented Industrial Data-Driven Modeling Under the Curse of Dimensionality. *IEEECAA J. Autom. Sin.* **2023**, *10*, 1445–1461. [CrossRef]
22. Zhu, Y.; Bradic, J. Breaking the Curse of Dimensionality in Regression. *arXiv* **2017**, arXiv:1708.00430.
23. Cheng, M.; Zhao, X.; Dhimish, M.; Qiu, W.; Niu, S. A Review of Data-Driven Surrogate Models for Design Optimization of Electric Motors. *IEEE Trans. Transp. Electrif.* **2024**. [CrossRef]
24. McNeish, D.M.; Stapleton, L.M. The Effect of Small Sample Size on Two-Level Model Estimates: A Review and Illustration. *Educ. Psychol. Rev.* **2016**, *28*, 295–314. [CrossRef]
25. Vabalas, A.; Gowen, E.; Poliakoff, E.; Casson, A.J. Machine Learning Algorithm Validation with a Limited Sample Size. *PLoS ONE* **2019**, *14*, e0224365. [CrossRef]
26. Kokol, P.; Kokol, M.; Zagoranski, S. Machine Learning on Small Size Samples: A Synthetic Knowledge Synthesis. *Sci. Prog.* **2022**, *105*, 00368504211029777. [CrossRef] [PubMed]
27. Balaci, A.T.; Suh, E.S.; Hwang, J. Systematic Application of Traffic-Signal-Control System Architecture Design and Selection Using Model-Based Systems Engineering and Pareto Frontier Analysis. *Syst. Eng.* **2024**. [CrossRef]
28. Cheikh, M.; Jarboui, B.; Loukil, T.; Siarry, P. A Method for Selecting Pareto Optimal Solutions in Multiobjective Optimization. *J. Inform. Math. Sci.* **2010**, *2*, 51–62.
29. Wang, N.; Zhao, W.; Wu, N.; Wu, D. Multi-Objective Optimization: A Method for Selecting the Optimal Solution from Pareto Non-Inferior Solutions. *Expert Syst. Appl.* **2017**, *74*, 96–104. [CrossRef]
30. Rao, R.V.; Lakshmi, R.J. Ranking of Pareto-Optimal Solutions and Selecting the Best Solution in Multi- and Many-Objective Optimization Problems Using R-Method. *Soft Comput. Lett.* **2021**, *3*, 100015. [CrossRef]
31. Bianchi, N.; Bolognani, S.; Frare, P. Design Criteria for High-Efficiency SPM Synchronous Motors. *IEEE Trans. Energy Convers.* **2006**, *21*, 396–404. [CrossRef]
32. Bianchi, N.; Bolognani, S. Design Techniques for Reducing the Cogging Torque in Surface-Mounted PM Motors. *IEEE Trans. Ind. Appl.* **2002**, *38*, 1259–1265. [CrossRef]

33. Ilina, I.-D.; Trifu, I.; Ghiţă, C.; Nedelcu, S. Influence of Design Parameters on the Cogging Torque of Permanent-Magnet Synchronous Generators. In Proceedings of the 2014 International Conference on Applied and Theoretical Electricity (ICATE), Craiova, Romania, 23–25 October 2014; pp. 1–6.
34. Farhani, F.; Zaafouri, A.; Chaari, A. Real Time Induction Motor Efficiency Optimization. *J. Frankl. Inst.* **2017**, *354*, 3289–3304. [CrossRef]
35. Papa, G.; Korousic-Seljak, B.; Benedicic, B.; Kmecl, T. Universal Motor Efficiency Improvement Using Evolutionary Optimization. *IEEE Trans. Ind. Electron.* **2003**, *50*, 602–611. [CrossRef]
36. Liu, M.; Zou, J.; Xu, Y.; Lan, H.; Yu, G. Vibration Enhancement or Weakening Effect Caused by Permanent Magnet Synchronous Motor Radial and Tangential Force Formed by Tooth Harmonics. *Energies* **2022**, *15*, 744. [CrossRef]
37. Wang, X.; Ye, P.; Zhang, Y.; Ni, H.; Deng, Y.; Lv, S.; Yuan, Y.; Zhu, Y. Parameter Optimization Method for Power System of Medium-Sized Bus Based on Orthogonal Test. *Energies* **2022**, *15*, 7243. [CrossRef]
38. Zhu, H.; Shen, S.; Wang, X. Multiobjective Optimization Design of Outer Rotor Coreless Bearingless Permanent Magnet Synchronous Motor. *IEEE J. Emerg. Sel. Top. Power Electron.* **2021**, *9*, 5489–5498. [CrossRef]
39. Ye, X.; Wu, L.; Sun, C.; Wang, L.; Zhang, J. Approximate Modeling of Gear Torque of Permanent Magnet Synchronous Motor Based on Improved Latin Hypercube Sampling. In *Proceedings of the 9th Frontier Academic Forum of Electrical Engineering*; Chen, W., Yang, Q., Wang, L., Liu, D., Han, X., Meng, G., Eds.; Springer: Singapore, 2021; pp. 487–500.
40. Wang, D.; Zhang, L.; Yang, F.; Yang, J.; Wu, Y.; Cao, P. Dynamic Response and Optimal Design of Radio Telescope Structure under Wind Load Excitation. *Buildings* **2023**, *13*, 2764. [CrossRef]
41. Xiao, Q.; Wang, J.; Jiang, B.; Yang, W.; Yang, X. Multi-Objective Optimization of Squirrel Cage Fan for Range Hood Based on Kriging Model. *Proc. Inst. Mech. Eng. Part C J. Mech. Eng. Sci.* **2022**, *236*, 219–232. [CrossRef]
42. Cheng, R.; Yu, J.; Zhang, M.; Feng, C.; Zhang, W. Short-Term Hybrid Forecasting Model of Ice Storage Air-Conditioning Based on Improved SVR. *J. Build. Eng.* **2022**, *50*, 104194. [CrossRef]
43. Li, R.; Xu, S.; Li, S.; Zhou, Y.; Zhou, K.; Liu, X.; Yao, J. State of Charge Prediction Algorithm of Lithium-Ion Battery Based on PSO-SVR Cross Validation. *IEEE Access* **2020**, *8*, 10234–10242. [CrossRef]
44. Bastos-Filho, C.J.A.; Miranda, P.B.C. Multi-Objective Particle Swarm Optimization Using Speciation. In Proceedings of the 2011 IEEE Symposium on Swarm Intelligence, Paris, France, 11–15 April 2011; pp. 1–6.

Disclaimer/Publisher's Note: The statements, opinions and data contained in all publications are solely those of the individual author(s) and contributor(s) and not of MDPI and/or the editor(s). MDPI and/or the editor(s) disclaim responsibility for any injury to people or property resulting from any ideas, methods, instructions or products referred to in the content.